Joel P. Felmlee, MS • Richard L. Ehman, MD

Spatial Presaturation: A Method for Suppressing Flow Artifacts and Improving Depiction of Vascular Anatomy in MR Imaging[1]

In clinical magnetic resonance (MR) imaging, the diagnostic quality of examinations is often degraded by streaklike flow artifacts that obscure anatomic details and reduce contrast. In addition, vascular structures are often not depicted clearly because the desired flow voids are obliterated by spurious intraluminal signals. On the basis of analysis of the physical mechanism of flow artifact formation, the authors developed a new technique for suppressing these artifacts. This applies interleaved, spectrally shaped radio frequency pulses to selectively saturate spins located in regions outside the image volume. In phantom, volunteer, and clinical imaging studies, the technique has proved to be effective by yielding a striking reduction in flow artifacts and markedly improving the reliability with which arterial and venous structures are imaged. The method has few drawbacks: It is applicable to most MR pulse sequences and, in principle, can be implemented on most imagers. It is particularly helpful for high-resolution surface coil studies of the neck, mediastinal imaging, gated cardiac imaging, and for detecting thrombus and other intravascular lesions such as dissections.

Index terms: Arteries, MR studies, 9.1214 • Blood vessels, MR studies • Magnetic resonance (MR), artifact • Magnetic resonance (MR), technology • Veins, MR studies, 9.1214

Radiology 1987; 164:559–564

In clinical magnetic resonance (MR) imaging, the diagnostic quality of examinations is often reduced by a variety of artifacts resulting from physiologic motion and blood flow (1–4). Strategies for reducing these artifacts have included gating techniques for cardiac, respiratory, and cerebrospinal fluid (CSF) motion (5–7), and other methods for reducing respiratory artifact (8). These techniques have been useful, but even when cardiac and respiratory artifacts are absent, MR images are frequently degraded by other artifacts. The most obvious of these are flow artifacts, which extend in a zipper-like fashion in the image from vessels passing through the plane of section (Fig. 1a). In conventional two-dimensional Fourier transform (2DFT) imaging, the artifacts radiate from vessels in the direction of the phase-encoding axis and can markedly obscure anatomic detail. We have observed that these artifacts are accentuated in high-resolution, small-field-of-view studies. They are very prominent when improvements in the signal-to-noise ratio gained by use of surface coils, high field strength, or other techniques are exploited to reduce imaging time by decreasing the amount of signal averaging. These artifacts often present major problems in imaging the neck and mediastinum.

A second problem is the inconsistency with which vascular lumens are often depicted on MR images. Many of the unique clinical applications that have been described for MR imaging take advantage of its ability to provide high contrast between flowing blood and stationary structures (9–24). Reliable detection

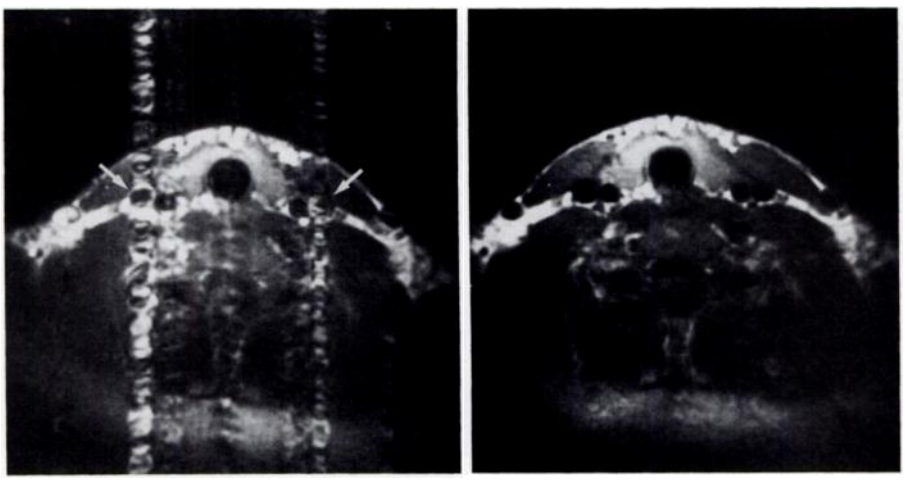

a. b.

Figure 1. Flow artifact reduction by spatial presaturation. **(a)** Surface coil MR image of cervical region acquired in 2 minutes, 34 seconds, with a standard sequence (repetition time [TR] = 600 msec, echo time [TE] = 30 msec, 256 views, one excitation, section one of seven 5-mm-thick sections). Multiple flow artifacts are present, arising predominantly from internal jugular veins (arrows) but also from common carotid arteries and external jugular veins. The lumens of the major vessels are poorly defined. **(b)** Surface coil image of same volunteer with spatial presaturation sequence acquired in same acquisition time and with same sequence parameters as in **a.** Note the almost complete absence of flow artifact and the clear depiction of vascular structures and surrounding tissues. The anatomy of the spinal canal and adjacent tissues is also better demonstrated because CSF pulsation artifact is suppressed.

[1] From the Department of Radiology, Mayo Clinic and Foundation, Rochester, MN 55905. From the 1986 RSNA annual meeting. Received December 4, 1986; revision requested February 5, 1987; revision received February 17; accepted April 7. **Address reprint requests to** R.L.E.

of vascular abnormalities such as thrombus, dissection, and lack of patency is critically dependent on consistent depiction of vascular lumens. Unfortunately, various flow phenomena result in intraluminal signals that degrade the uniform flow void and thereby obscure or simulate intraluminal pathologic areas. We have had difficulty with the consistency and reliability of MR imaging for some of its most frequently touted vascular applications because of these problems.

Our analysis of the physical principles underlying these flow artifact phenomena led to a possible method for eliminating "zipper" artifact and improving the depiction of flow voids that has not, to our knowledge, been previously described. Our hypothesis was that by properly controlling the spatial distribution of longitudinal magnetization outside the volume of tissue that is imaged, these artifacts can be suppressed.

The purpose of this project was to develop and test this method for eliminating flow artifacts and to explore its clinical applications. The method is based on application of additional spectrally shaped radio frequency (RF) pulses during imaging to saturate or invert spins that are located outside the volume of tissue that is being imaged.

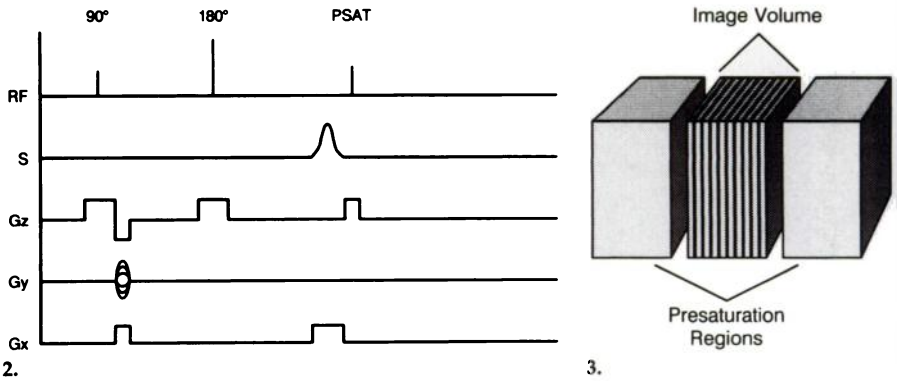

Figures 2, 3. **(2)** Pulse sequence for single-axis spatial presaturation. The presaturation selection can be accomplished with any of the section-selection, phase-encoding, or frequency-encoding gradients shown. The "*PSAT*" pulse indicates the spectrally shaped RF pulse used to excite regions external to the image volume. The sequence shown is repeated for each image within a multisection study. Since the PSAT spectral content remains constant, the effective TR within the presaturation regions is TR/*N* for an *N*-section acquisition. **(3)** Position of the image volume and presaturation regions. The image volume is defined by the boundaries of the acquired images. For the single-axis case, the presaturation regions are positioned on each side of the image volume. Although presaturation along the section-selection direction is shown, presaturation regions could have been positioned along the phase- or frequency-encoding axes as well.

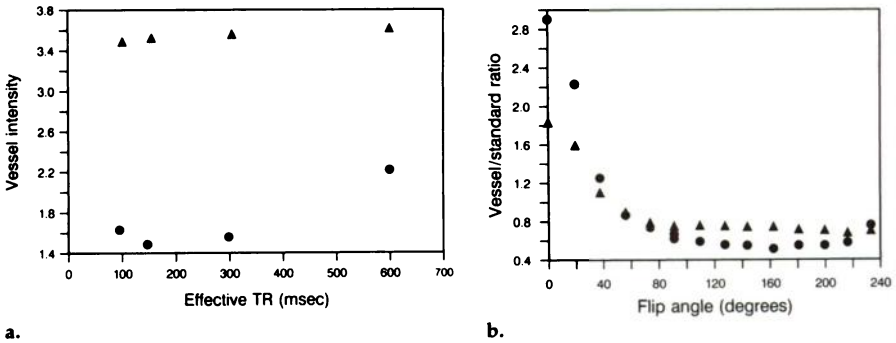

Figure 4. Flow intensity reduction by spatial presaturation. **(a)** The entrance section intensity of a flow channel containing 1.0 mM cupric sulfate solution with an average velocity of 5 cm/sec, on images acquired with and without spatial presaturation (TR = 600 msec, TE = 30 msec, 128 views, one excitation, 10-mm-thick sections, 90° presaturation nutation angle), is plotted versus effective TR within the presaturation regions. ▲ = presaturation off, ● = presaturation on. **(b)** The ratio of flow channel intensity to static standard intensity is plotted versus nutation angle within the presaturation region. Cupric sulfate solution of the same concentration was used for the static standard. (Image sequence parameters as in **a**, seven-section acquisition, effective TR = 86 msec.) ● = 5 cm/sec, ▲ = 11 cm/sec.

MATERIALS AND METHODS

The pulse-control software of standard multisection, multiecho sequences for a 1.5-T imager (General Electric, Milwaukee) was modified to incorporate extra gradient waveforms and spectrally shaped RF pulses as shown in Figure 2. These RF pulses (typically 3 msec long) were designed to selectively saturate spins in regions exterior to the image volume, as shown in Figure 3. The spectral content of the RF pulses was determined by the location and dimensions of the desired presaturation regions and was constant during image acquisition. Therefore, the presaturation regions received one nutation pulse for each image acquired during a multisection acquisition. Note that these modifications did not increase imaging time.

Phantoms were constructed to evaluate the effect of presaturation on pulsatile flowing fluids. Flow channels measuring 12 mm in diameter were positioned longitudinally in the imager, adjacent to static reference standards containing 1.3 mM cupric sulfate solution. Pulsatile flow of the same solution was provided by a hemodialysis displacement pump (Drake and Willock, Portland, Ore.). Average flow velocities of 5 cm/sec and 11 cm/sec were provided at pulse frequencies of 55/min and 100/min. The estimated peak velocities were 20 cm/sec and 44 cm/sec, respectively.

Flow phantom experiments were conducted to evaluate the effect of presaturation on the intensity of the flow channel and zipper artifacts. Comparison images were acquired with and without presaturation RF pulses with seven-section acquisition, 10-mm image section thickness, 30-msec TE, and 600-msec TR. Intensities were measured in appropriate regions of interest in each image. We assessed the influence of the following factors on flow channel and artifact intensity: "effective TR" of the presaturation region, presaturation nutation angle, presaturation region thickness, presaturation region to image volume gap, and interimage gap. In addition, the delivery of presaturation RF by singular (two presaturation regions excited individually) or composite (two presaturation regions excited simultaneously) excitation methods was evaluated.

Volunteers were imaged with and without presaturation RF excitation pulses to evaluate the ability of the technique to improve the depiction of vascular anatomy and suppressing flow artifacts in vivo.

After testing on phantoms and volunteers, the presaturation sequences were used in selected clinical examinations. The presaturation technique was also incorporated into pulse control software for gated cardiac imaging.

RESULTS

Evaluation of the presaturation technique in phantom and volunteer studies demonstrated striking reduc-

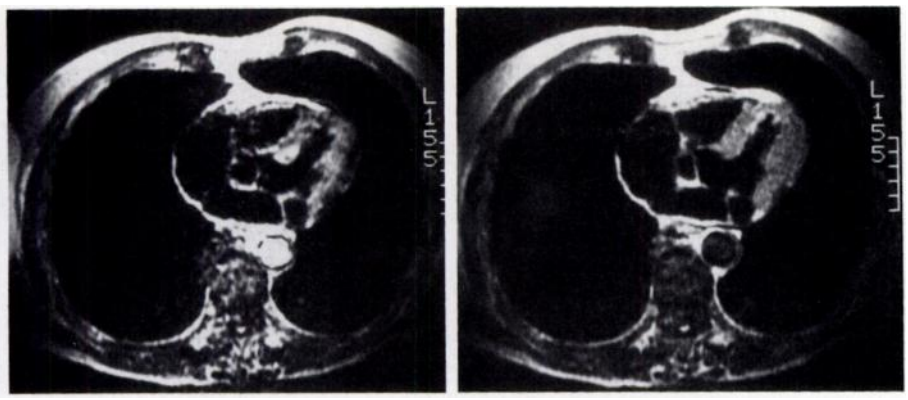

a. b.

Figure 5. Gated cardiac images (middle section of seven-section acquisition). **(a)** Standard spin-echo sequence yields a cardiac image with considerable flow artifact, which is especially apparent over the spine. **(b)** Presaturation image demonstrates much less flow artifact, along with more uniform myocardial intensity, darker myocardial chambers, and a much better flow void in the descending aorta.

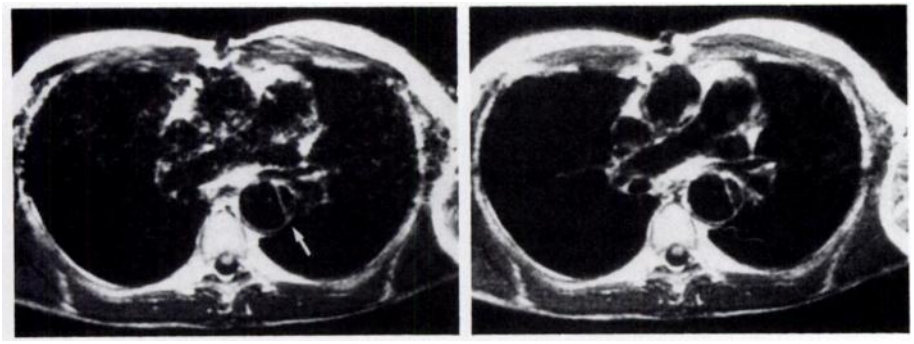

a. b.

Figure 6. Mediastinum. **(a)** Image acquired without spatial presaturation. Note that the phase-encoding axis is positioned horizontally so that the flow artifacts propagate laterally. The patient has an aortic dissection with an intimal flap in the descending aorta (arrow). **(b)** The same patient imaged with spatial presaturation. Note the decreased flow-related artifacts and improved depiction of the mediastinal vascular anatomy.

tion of flow artifacts and marked improvement in the depiction of vascular anatomy (Fig. 1b). The phantom studies demonstrated that the intensity of the lumen of the flow channel was typically reduced by more than a factor of two in the boundary sections, where luminal enhancement and flow artifact is usually most intense. The intensity of the flow artifacts decreased in direct proportion to the reduction of intensity in the flow channel (typical correlation, .995). The improvement was not limited to the outer sections only. For example, with typical pulsatile flow (peak velocity of 44 cm/sec) the presaturation technique reduced artifact intensities by 86%, 80%, 63%, and 47% in four sections from the edge to the middle of the image volume, respectively. The effect of presaturation repetition time and nutation angle is shown in Figure 4.

The flow phantom studies also demonstrated that the following interventions had relatively little influence on the presaturation effectiveness: varying the presaturation region thickness (4, 8, or 16 cm), changing the gap between the presaturation region and the image volume (0, 1, or 2 cm), and varying the gap between image sections (0, 0.5, and 1.0 cm). Singular and composite presaturation RF pulses provided essentially identical results.

Gated cardiac imaging in volunteers consistently demonstrated marked improvement with the presaturation technique (Fig. 5). Again, the improvement was due to a reduction in flow artifact and an improvement in the blackness of the flow voids in vessels and cardiac chambers. Clinical examinations demonstrated similar results (Fig. 6). In most cases, the presaturation technique increased the diagnostic quality of the examinations by yielding a more reliable depiction of vascular anatomy, with fewer spurious intraluminal signals.

DISCUSSION

The first step in coping with artifact phenomena in MR imaging is to define the physical mechanisms. Zipperlike flow artifacts arise because of temporal variations in the transverse magnetization in volume elements within blood vessels during image acquisition. Pulsatile flow can cause view-to-view modulation of both the magnitude and the average phase angle of the quadrature spin-echo signal elicited from each voxel. These two kinds of variation can have similar effects on the 2DFT reconstruction process, resulting in similar zipper artifacts.

Phase modulation results from a well-known effect, in which flow or motion in the presence of a magnetic gradient causes a phase shift in the precessing magnetization vector that is in many cases proportional to the velocity and the strength of the gradient (25–31). If a wide distribution of velocities is present within a volume element, there will be a wide distribution of phase angles and the vector sum of the signals will be reduced. This process of phase dispersion within a volume element is partly responsible for the "flow-void" phenomenon but is not a cause of flow artifact formation. Rather, flow artifacts resulting from phase modulation are due to narrower distributions of phase shifts resulting from bulk motion with a relatively narrow distribution of velocities within volume elements. The spin-echo signal from these volume elements is not attenuated because the vector sum adds more coherently, but the net phase angle of the signal from the volume element is shifted. This nondispersive phase shift typically varies from view to view due to the pulsatile and pseudoperiodic nature of physiologic flow. This defeats the 2DFT localization process and causes mismapping of signals originating from vascular lumens to other locations along the phase axis (2, 3, 32).

View-to-view amplitude modulation of the net voxel magnetization vector due to pulsatile flow can result from variation in the degree of intensity loss due to phase dispersion. It is also caused by view-to-view differences in the quantity of relatively unsaturated spins that are washed into the imaging volume (flow-related enhancement).

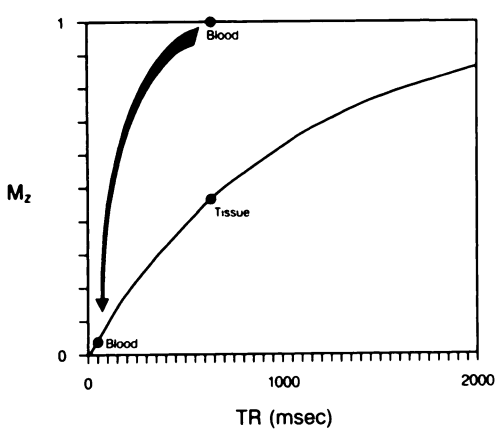

7.

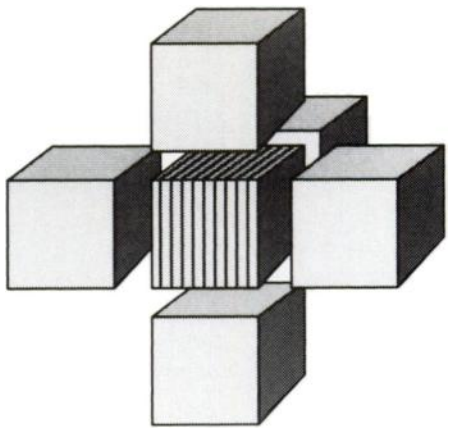

8.

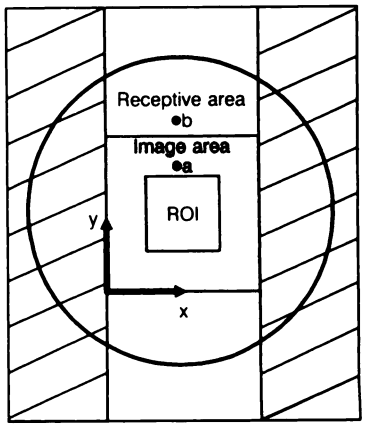

9.

Figures 7-9. **(7)** Schematic representation of the status of longitudinal magnetization in blood and adjacent stationary tissue. If the tissue was imaged at a TR of 650 msec as shown and ten sections were acquired, the effective TR in the presaturation regions would be one-tenth of this value. The longitudinal magnetization of unsaturated blood in the standard situation is shown. With presaturation, the longitudinal magnetization of blood entering the image volume can be markedly reduced, as indicated by the arrow. **(8)** Cut-away schematic of the three-axis spatial presaturation technique. The image volume is centered within presaturation regions selected along the section-selection, phase-encoding, and frequency-encoding directions. **(9)** Diagram indicating the circular receptive area of the receiver coil, the image area determined by the phase- and frequency-encoding gradients, and the clinical region of interest within the image area. The hatched regions indicate regions from which spurious signals can be filtered electronically if frequency encoding is along the x-axis. Objects in the unhatched regions outside the image area will be projected into the image due to the aliasing or wraparound effect.

Several approaches have been proposed for dealing with flow artifacts. Displacement of flow artifacts away from important areas in images is often possible by careful selection of the direction of the phase-encoding axis, but this is at best a limited solution. The so-called gradient-moment nulling or flow-compensation techniques are among the most promising (33–36). These techniques adjust the strength and duration of imaging gradients so as to minimize the net phase accumulation of flowing blood. This clearly reduces the amount of view-to-view phase modulation. Unfortunately, the technique only partially addresses the problem of amplitude modulation, since it will correct only the view-to-view intensity variation caused by phase dispersion and not the component caused by flow-related enhancement. A more fundamental problem is that by allowing the reconstruction process to map correctly the intensity of flowing blood to the vascular lumen and by eliminating attenuation due to phase dispersion, this method inevitably leads to depiction of vascular lumens with high signal intensity rather than as flow voids. This tends to obscure important intraluminal abnormalities such as dissections, tumors, and thrombi. It also tends to reduce the contrast between small vascular structures and surrounding tissue.

Our analysis of the phenomena of flow artifacts and flow-void degradation indicates that flow-related enhancement can be regarded as the basic problem. If flowing spins could be properly saturated so that their longitudinal magnetization is very small when they enter the plane of section, then vascular lumens would be depicted with low intensity. Furthermore, flow artifact zippers would also be suppressed because, regardless of the degree of phase modulation, there would be little signal power to mismap in the image. Flow artifacts are also suppressed by this intervention because view-to-view intensity modulation would be eliminated. The hypothesis that a lack of saturation of flowing spins is the most basic problem is supported by the well-known observation that flow artifacts seem to be a greater problem in high-field-strength imagers. This is partly due to that fact that less signal averaging is typically used, which makes the artifacts more apparent. But the basic reason is that at a given TR, tissues are more saturated at high field strength than at low field strength because the T1 relaxation times are longer. This means that the degree of unsaturation of blood that flows into the plane of section from outside the image volume is greater at high field strengths, and therefore the degree of flow void degradation and flow artifact formation is greater.

The approach that we have developed to minimize flow artifacts employs additional spatially selective RF pulses to saturate spins that are outside the volume that is imaged during multisection acquisition. Spins that flow into the image volume must pass through these presaturation regions. The presaturation pulses are applied to the same regions every time a section is interrogated. Thus, for a multisection acquistion with a given TR, in which N sections are acquired, the effective TR in the presaturation regions is TR/N. Stationary spins within the presaturation regions will thus be extremely saturated. Depending on the flow velocity, blood passing through the presaturation regions into the image volume will be subjected to several presaturation pulses. Slow-flowing blood, which tends to cause the greatest amount of flow-related enhancement, will be subject to the greatest amount of presaturation. In any case, the blood entering the imaging volume is likely to be more saturated than stationary spins within image sections. This "supersaturation" effect means that the contrast between vascular lumens and surrounding tissue will be improved more than if flow-related enhancement were simply eliminated (Fig. 7).

Incorporation of presaturation pulses into current imaging sequences carries few penalties. The additional RF irradiation does increase the energy deposition of the sequence, which can be an issue with high-field-strength imagers. However, the additional energy deposition associated with the method that has been described is only one-half that associated with addition of a single

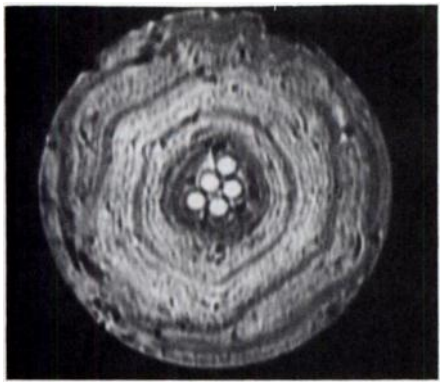

a.

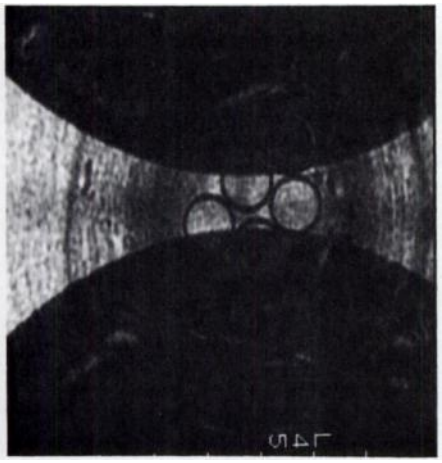

b.

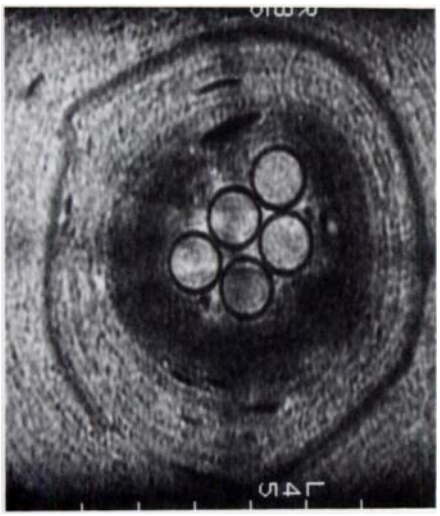

c.

Figure 10. Application of presaturation to suppress aliasing. **(a)** Large field-of-view image of a cylindrical phantom. **(b)** High-resolution image of the phantom in which the dimensions of the field of view are less than the diameter of the phantom. The overlapping low-intensity areas are due to aliasing or wraparound. The phase-encoding axis is vertical in this image. **(c)** Second acquisition with same field of view as in **b** but with use of presaturation. The presaturation regions have been placed laterally to suppress the signal from the portions of the phantom that are outside the field of view. This has markedly reduced the amount of aliasing artifact. The nutation angle within the presaturation regions was 135°.

additional spin echo to the sequence. A second possible disadvantage is that the cycle time for acquisition of each view is increased slightly, on the order of 3–6 msec. However, with composite RF presaturation pulses, this time can be reduced and they can potentially be placed in "free time" between echoes, so that no net increase in cycle time is created. Alternatively, the composite presaturation pulses could be applied during the short-duration refocusing gradient lobes required by some imaging sequences, or even incorporated into the preexisting 90° or 180° imaging pulses for a similar effect.

The method described to this point is effective only for flow that is predominantly along the section-selection axis. This is a common but not constant geometry in clinical imaging. In certain situations, such as coronal imaging of the body, presaturation along the frequency or phase axes may be appropriate and is easily implemented. In the general case, unsaturated spins may enter the image volume from any direction, and in this context, a three-axis presaturation technique is appropriate (Fig. 8). This technique was implemented by extension of the single-axis method and is particularly applicable to cardiac imaging.

We have found that the three-axis presaturation technique has other interesting applications in addition to flow artifact suppression. It can also be used to reduce motion and aliasing artifacts by saturating and thereby suppressing signals from areas within the receptive area of the receiver coil but outside the clinical region of interest. In Figure 9, object *a* could be the anterior abdominal wall in a transaxial spinal imaging examination. Motion from this structure during image acquisition creates artifacts, which degrade the image quality within the region of interest. By placing a presaturation region over the moving structures, their signal can be suppressed, thereby minimizing the motion artifacts.

When an extended object is imaged with the 2DFT technique, the phenomenon of aliasing limits the extent to which spatial resolution can be increased by strengthening the frequency- and phase-encoding gradients. In Figure 9, object *b* lies outside the image area, which is defined in the y direction by the maximum phase-encoding gradient amplitude. In the final image, this object will appear within the image area, near its lower margin, because of aliasing or "wraparound." A similar object located in the hatched regions to the right and left of the image area will typically not show aliasing artifact because its false signal can be filtered electronically.

Figure 10 demonstrates an application of presaturation for suppressing aliasing along the phase-encoding axis. We have observed that when presaturation is used to suppress motion and aliasing artifact, the effectiveness is improved when the nutation angle in the presaturation regions is increased beyond 90°. This is in contrast to flow-artifact suppression applications, in which larger nutation angles were not particularly advantageous (Fig. 4b). The short T1 of subcutaneous fat precludes effective saturation, but inverting pulses can exploit the intensity-nulling capability of inversion recovery by arranging the section interrogation to occur at the zero crossing of the longitudinal magnetization in the presaturation region.

Several other applications of spatial presaturation seem attractive. This approach can be incorporated into imaging sequences with gradient-refocussed, fast-imaging techniques. Presaturation may provide a novel method for projective MR angiography, for which several methods have already been proposed (37, 38). Two images could be obtained, one with and one without spatial presaturation. Subtraction of these images would yield an image in which the stationary tissue signals are suppressed, leaving only the enhanced vascular structures. We speculate that application of flow compensation gradient techniques to the nonpresaturated image would improve the method. Spatial presaturation may also provide a new approach for spatially resolved spectroscopy by suppressing the signal from unwanted regions (39).

As a clinical tool, this technique has already assumed an important role in our practice. We have found it particularly helpful in surface coil examinations with small fields of view and high spatial resolution, where the reduction of flow artifact can be striking. It is used in any case in which intraluminal abnormality such as tumor, dissection, or thrombus is suspected. The technique is helpful for differentiating flow-related enhancement from thrombus. It is used in any examination in which high vascular conspicuity is needed, such as delineating the relation of intrahepatic vessels to liver tumors pri-

or to attempted resection.

Spatial presaturation can, in principle, be implemented on any imager. It does not increase imaging time or limit the choice of parameters such as TR or TE. In clinical imaging we have found that the most important application of this technique is to suppress flow artifacts and to improve the reliability with which vascular structures are depicted. ■

Acknowledgments: We are grateful for the support of our colleagues in this work, especially Paul R. Julsrud, M.D., Thomas H. Berquist, M.D., and Joel E. Gray, Ph.D. (Department of Radiology, Mayo Clinic and Foundation). We also gratefully acknowledge the technical assistance provided by Ann Shimakawa, M.S., and Joseph K. Maier, M.S. (General Electric Medical Systems).

References

1. Axel L, Sommers RM, Kressel HY, Charles C. Respiratory effects in two dimensional Fourier transform MR imaging. Radiology 1986; 160:795–801.
2. Ehman RL, McNamara MT, Brasch RC, Felmlee JP, Gray JE, Higgins CB. Influence of physiologic motion on the appearance of tissue in MR images. Radiology 1986; 159:777–782.
3. Perman WH, Moran PR, Moran RA, Bernstein MA. Artifacts from pulsatile flow in MR imaging. J Comput Assist Tomogr 1986; 10:473–483.
4. Shultz CL, Alfidi RJ, Nelson AD, Kopiwoda SY, Clampitt ME. The effect of motion on two-dimensional Fourier transformation magnetic resonance images. Radiology 1984; 152:117–121.
5. Lanzer P, Botvinick EH, Schiller NB, et al. Cardiac imaging using gated magnetic resonance. Radiology 1984; 150:121–127.
6. Ehman RL, McNamara MT, Pallack M, Hricak H, Higgins CB. Magnetic resonance imaging with respiratory gating: techniques and advantages. AJR 1984; 143:1175–1182.
7. Bergstrand G, Bergstrom M, Nordell B, et al. Cardiac gated MR imaging of cerebrospinal fluid flow. J Comput Assist Tomogr 1985; 9:1003–1006.
8. Bailes DR, Gilderdale DJ, Bydder GM, Collins AG, Firmin DN. Respiratory ordered phase encoding (rope): a method for reducing respiratory motion artifacts in MR imaging. J Comput Assist Tomogr 1985; 9:835–838.
9. Kaufman L, Crooks LE, Sheldon PE, Rowan W, Miller T. Evaluation of NMR imaging for detection and quantification of obstructions in vessels. Invest Radiol 1982; 17:554–560.
10. Herfkins RJ, Higgins CB, Hricak H, et al. Nuclear magnetic resonance imaging of the cardiovascular system: normal and pathological findings. Radiology 1983; 147:749–759.
11. Lee JK, Ling D, Heiken JP, et al. Magnetic resonance imaging of abdominal aortic aneurysms. AJR 1984; 143:1197–1202.
12. Amparo EG, Higgins CB, Hoddick W, et al. Magnetic resonance imaging of aortic disease: preliminary results. AJR 1984; 143:1203–1209.
13. Amparo EG, Hoddick WK, Hricak H, et al. Comparison of magnetic resonance imaging and ultrasonography in the evaluation of abdominal aortic aneurysms. Radiology 1985; 154:133–136.
14. Geisinger MA, Rissius B, O'Donnel JA, et al. Thoracic aortic dissections: magnetic resonance imaging. Radiology 1985; 155:407–412.
15. Flak B, Li BK, Ho BY, et al. Magnetic resonance imaging of aneurysms of the abdominal aorta. AJR 1985; 144:991–996.
16. Higgins CB, Byrd BF, McNamara MT, et al. Magnetic resonance imaging of the heart: a review of the experience in 172 subjects. Radiology 1985; 155:671–679.
17. Hricak H, Amparo E, Fisher MR, Crooks L, Higgins CB. Abdominal venous system: assessment using MR. Radiology 1985; 156:415–422.
18. Wesbey GE, Higgins CB, Amparo EG, Hale JD, Kaufman L, Pogany AC. Peripheral vascular disease: correlation of MR imaging and angiography. Radiology 1985; 156:733–739.
19. Glazer HS, Gutierrez FR, Levitt RG, Lee JK, Murphy WA. The thoracic aorta studied by MR imaging. Radiology 1985; 157:149–155.
20. Williams DM, Cho KJ, Aisen AM, Eckhauser FE. Portal hypertension evaluated by MR imaging. Radiology 1985; 157:703–706.
21. Bernardino ME, Steinberg HV, Pearson TC, Gedgaudas-McClees RK, Torres WE, Henderson JM. Shunts for portal hypertension: MR and angiography for determination of patency. Radiology 1986; 158:57–61.
22. Goldberg HI, Grossman RI, Gomori JM, Asbury AK, Bilaniuk LT, Zimmerman RA. Cervical internal carotid artery dissecting hemorrhage: diagnosis using MR. Radiology 1986; 158:157–161.
23. von Schulthess GK, Higashino SN, Higgins SS, Didier D, Fisher MR, Higgins CB. Coarctation of the aorta: MR imaging. Radiology 1986; 158:469–474.
24. McMurdo KK, de Geer G, Webb WR, Gamsu G. Normal and occluded mediastinal veins: MR imaging. Radiology 1986; 159:33–38.
25. Singer JR. NMR diffusion and flow measurements and an introduction to spin phase graphing. Phys E Sci Instrum 1978; 11:281–291.
26. Moran PR, Moran RA, Karstaedt N. Verification and evaluation of internal flow and motion. Radiology 1985; 154:433–441.
27. Axel L. Blood flow effects in magnetic resonance imaging. AJR 1984; 143:1157–1166.
28. Bradley WG, Waluch V. Blood flow: magnetic resonance imaging. Radiology 1985; 154:443–450.
29. Wehrli FW, MacFall JR, Axel L, Shutts D, Glover GH, Herfkins RJ. Approaches to in-plane and out-of-plane flow imaging. Noninvasive Med Imaging 1984; 1:127–136.
30. Valk PE, Hale JD, Crooks LE, et al. MRI of blood flow: correlation of image appearance with spin echo phase shift and signal intensity. AJR 1986; 146:931–939.
31. Bradley WG, Waluch V, Lai K, Fernandez EJ, Spalter C. The appearance of rapidly flowing blood on magnetic resonance images. AJR 1984; 143:1167–1174.
32. Ehman RL, Felmlee JP, Houston DS, Julsrud PR, Gray JE. Nondispersive phase shifts caused by bulk motion and flow: significance for MR imaging (abstr.). In: Book of abstracts: Society of Magnetic Resonance in Medicine, 1986. Vol. 4. Berkeley, Calif.: Society of Magnetic Resonance in Medicine, 1986; 1099–1100.
33. Oh CH, Ra JB, Hilal SK, Cho ZH. A flow artifact correction method for multislice magnetic resonance imaging (abstr.). In: Book of abstracts: Society of Magnetic Resonance in Medicine, 1986. Vol. 1. Berkeley, Calif.: Society of Magnetic Resonance in Medicine, 1986; 133–134.
34. Axel L, Morton D. Blood flow imaging by velocity compensated/uncompensated phase subtraction (vcups) (abstr.). In: Book of abstracts: Society of Magnetic Resonance in Medicine, 1986. Vol. 1. Berkeley, Calif.: Society of Magnetic Resonance in Medicine, 1986; 104–105.
35. Lenz GW, Haacke EM, Nelson AD. High resolution, high signal to noise, flow quantification and vascular imaging (abstr.). In: Book of abstracts: Society of Magnetic Resonance in Medicine, 1986. Vol. 1. Berkeley, Calif.: Society of Magnetic Resonance in Medicine, 1986; 88–89.
36. Chenevert TL, Borrello JA. Flow enhanced imaging using flow corrective gradients (abstr.). In: Book of abstracts: Society of Magnetic Resonance in Medicine, 1986. Vol. 1. Berkeley, Calif.: Society of Magnetic Resonance in Medicine, 1986; 96–97.
37. Meuli RA, Wedeen VJ, Geller SC, et al. MR gated subtraction angiography: evaluation of lower extremities. Radiology 1986; 159:411–418.
38. Dumoulin CL, Hart HR. Magnetic resonance angiography. Radiology 1986; 161:717–720.
39. Luyten PR, den Hollander JA. Observation of metabolites in the human brain by MR spectroscopy. Radiology 1986; 161:795–798.